JHB

Journal of Health and Biology

https://journalhb.org/

SPBH

Original Article

Green Biosynthesis of Gold Nanoparticles Using Lactobacillus Species: Characterization and Antifungal Efficacy Evaluation

Maryam Jabbar Nasser [1]

[1] Department of Biology, College of Science, University of Al-Qadisiyah, Diwaniya, Iraq

Corresponding author: Maryam Jabbar Nasser, maryam.jabbar@qu.edu.iq

DOI: https://doi.org/10.71428/JHB.2026.0110

ABSTRACT

In recent years, the biological route for producing metallic nanoparticles has attracted considerable attention, mainly because it is eco-friendly and relatively low in cost when compared to the traditional physical and chemical approaches. The present study reports the green biosynthesis of gold nanoparticles (AuNPs) using the cell-free supernatant of a Lactobacillus species, and then evaluates their antifungal activity against selected pathogenic fungi. The bacterial isolate was cultivated in MRS broth, and its supernatant was obtained by centrifugation and mixed with 1 mM chloroauric acid (HAuCl4) under mild conditions. A gradual shift in color from pale yellow to ruby-red was noticed after a few hours, giving the first visual indication of nanoparticle formation. The biosynthesized AuNPs were characterized by UV-Vis spectroscopy, Fourier-transform infrared spectroscopy (FTIR), X-ray diffraction (XRD), and field emission scanning electron microscopy (FESEM). UV-Vis showed a typical surface plasmon resonance band near 535 nm, FTIR indicated the involvement of proteins and other biomolecules as capping/reducing agents, while XRD confirmed the face-centered cubic structure of metallic gold. FESEM images revealed nearly spherical particles with an average size ranging between 20 and 45 nm. The antifungal evaluation, carried out against *Candida albicans*, *Aspergillus niger,* and *Aspergillus flavus* by the agar well diffusion method, showed considerable inhibition zones, with minimum inhibitory concentration (MIC) values between 32 and 128 µg/mL. These findings suggest that Lactobacillus-mediated AuNPs can be regarded as a promising antifungal agent with potential biomedical applications.

Highlights

- AuNPs were successfully synthesized using a cell-free supernatant of Lactobacillus sp.
- The process was simple, rapid, and carried out without any toxic chemicals.
- FTIR, XRD, and FESEM confirmed the formation of crystalline, nearly spherical AuNPs.
- The nanoparticles displayed clear antifungal activity against Candida and Aspergillus species.
- MIC values ranged between 32 and 128 µg/mL depending on the tested fungal strain.

KEYWORDS: Gold nanoparticles; Lactobacillus; Green synthesis; Antifungal activity; Candida albicans; Aspergillus.

Received: January 21, 2026. Accepted: April 4, 2026. Published: May 12, 2026

Graphical Abstract

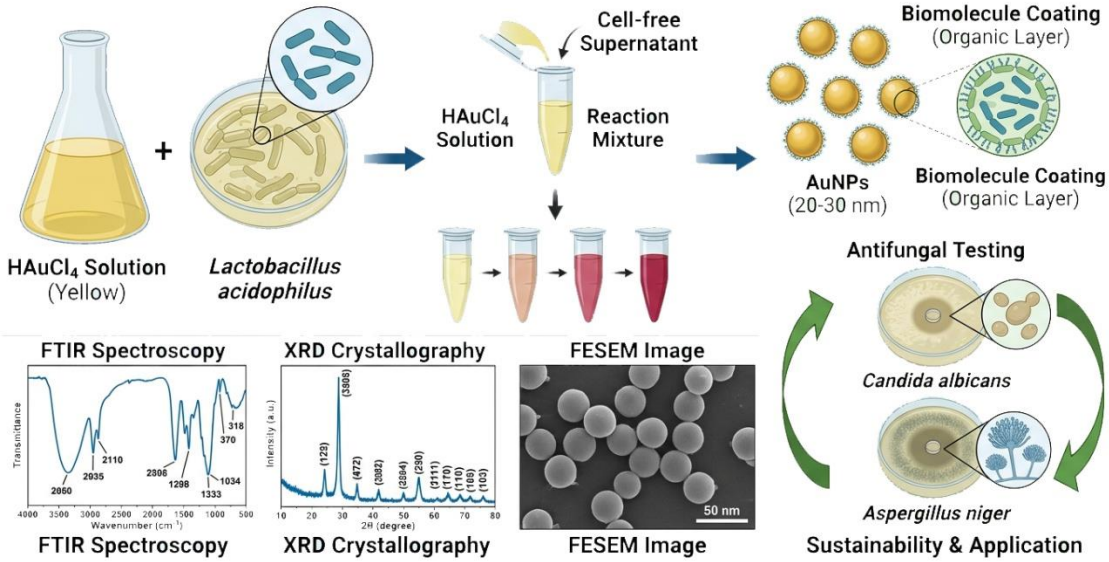

1. INTRODUCTION

Nanotechnology has emerged during the last two decades as one of the most active fields of applied science, providing new tools for medicine, agriculture, the food industry, and environmental remediation [1]. Among the various classes of nanomaterials, gold nanoparticles (AuNPs) occupy a distinguished position, thanks to their unique optical properties, high surface-to-volume ratio, and good biocompatibility, which together make them suitable for biosensing, imaging, drug delivery, and antimicrobial applications [2]. Traditionally, AuNPs are prepared by physical and chemical methods, yet most of these approaches depend on costly instruments or hazardous reducing agents, such as sodium borohydride and hydrazine, factors that considerably limit their biomedical use [3].

Green synthesis, which uses plants, fungi, and bacteria, has therefore been proposed as a safer and more sustainable alternative. Microbial-based strategies are especially attractive because microorganisms can be cultivated under controlled laboratory conditions, and their metabolic products behave as both reducing and stabilizing agents [4]. Lactobacillus species, in particular, are well-known probiotic bacteria that are generally regarded as safe (GRAS). Their cells and metabolites are rich in proteins, organic acids, peptides, and exopolysaccharides, all of which can reduce metal ions and later cap the resulting nanoparticles [5, 6].

On the other hand, fungal infections have become a serious clinical problem during the last few years, particularly those caused by Candida albicans and various Aspergillus species, mostly due to the increasing resistance to conventional antifungal drugs [7]. Accordingly, the search for alternative antifungal agents derived from bio-nanomaterials is growing quickly.

The present work was designed with three main aims: to biosynthesize AuNPs using the cell-free supernatant of a Lactobacillus isolate, to characterize the produced particles using UV-Vis, FTIR, XRD, and FESEM, and finally to evaluate their antifungal efficacy against selected human pathogenic fungi.

2. MATERIALS AND METHODS

2.1. Chemicals and biological materials

Chloroauric acid (HAuCl4·3H2O, ≥99%) was purchased from Sigma-Aldrich (USA). De Man, Rogosa, and Sharpe (MRS) broth and potato dextrose agar (PDA) were obtained from HiMedia

(India). Fluconazole discs (25 µg), used as a positive control, were supplied by a local medical distributor. Sterile distilled water was employed throughout all the experiments.

2.2. Bacterial strain and preparation of cell-free supernatant

A reference strain of Lactobacillus sp. was obtained from the microbiology laboratory at the College of Science. The strain was inoculated into sterile MRS broth and incubated anaerobically at 37 °C for 48 h. After incubation, the culture was centrifuged at 8000 rpm for 15 min at 4 °C. The clear supernatant was then filtered through a 0.22 µm syringe filter to ensure that no residual cells were carried over, and was used directly for the biosynthesis step.

2.3. Green biosynthesis of gold nanoparticles

The biosynthesis was performed following a modification of the protocol described by Markus et al. [8]. Briefly, 10 mL of the cell-free supernatant was added dropwise to 90 mL of 1 mM HAuCl4 solution under continuous magnetic stirring at room temperature. The pH of the reaction mixture was adjusted to 7.0 using 0.1 M NaOH. The reaction was then allowed to proceed for up to 24 h in the dark, in order to minimize photo-induced reduction. The formation of AuNPs was monitored first by visual inspection of the color change from pale yellow to reddish-purple, and later by UV-Vis spectroscopy. The resulting colloid was centrifuged at 12,000 rpm for 20 min; the pellet was washed three times with deionized water, air-dried, and finally kept in a desiccator until further use.

2.4. Characterization techniques

The optical properties of the biosynthesized AuNPs were analyzed using a UV-Vis spectrophotometer (Shimadzu UV-1800, Japan) in the wavelength range of 300–700 nm. FTIR spectra were recorded between 4000 and 400 cm-1 on a Bruker FTIR spectrometer, in order to identify the functional groups involved in the reduction and capping processes. The crystalline structure of AuNPs was examined using XRD (Philips X'Pert, Netherlands) with Cu-Kα radiation (λ = 1.5406 Å), scanning the 2θ range 20°–80°. Field emission scanning electron microscopy (FESEM) coupled with energy-dispersive X-ray spectroscopy (EDX) was used to investigate the morphology, particle size distribution, and elemental composition.

2.5. Test fungi

Three pathogenic fungi were used for the antifungal assay: *Candida albicans* (ATCC 10231), *Aspergillus niger,* and *Aspergillus flavus*. All isolates were identified at the Mycology Unit and were sub-cultured on PDA prior to use in order to guarantee the purity and viability of the strains.

2.6. Antifungal activity assay

Biosynthesised AuNPs were tested for antifungal activity using the agar well diffusion method suggested by Balouiri *et al.* [9], with minor modifications. A spore suspension (about 1.5×10^{6}CFU/mL) of each fungus was evenly distributed on PDA plates. With a sterile cork borer, 6 mm wells were punched in the agar. Various AuNP concentrations (25, 50, 100, and 200µg/mL) were diluted in sterile distilled water, and 100µL was placed into each well. A fluconazole disc (25µg) was used as a positive control, and sterile distilled water served as the negative control. Plates were incubated at 28 °C for 48–72 h, after which the inhibition zones were measured in millimeters using a digital caliper. All experiments were carried out in triplicate.

2.7. MIC and MFC determination

Minimum inhibitory concentration (MIC) was determined by the broth microdilution method, using serial two-fold dilutions of AuNPs in Sabouraud dextrose broth. The minimum fungicidal concentration (MFC) was then identified by sub-culturing 10 µL of broth from each clear well onto fresh PDA plates; MFC was defined as the lowest concentration at which no visible fungal growth appeared after incubation.

2.8. Statistical analysis

All data were expressed as mean ± standard deviation (SD) of three independent replicates. One-way ANOVA followed by Duncan's multiple range test was applied using SPSS v.25 (IBM, USA). Differences were considered statistically significant at $p < 0.05$.

3. RESULTS AND DISCUSSION

3.1. Visual observation and UV-Vis spectroscopy

Soon after the Lactobacillus supernatant was added to the chloroauric acid solution, the color of the mixture started to change slowly. After about 2 h, the solution turned pale pink, and within 12–24 h it reached a clear ruby-red color. Such a color shift is commonly regarded as the first visual evidence of AuNPs formation, and it arises from the excitation of surface plasmon resonance (SPR) of colloidal gold particles [10]. No color change was observed in the control (HAuCl4 alone), which rules out the possibility of chemical reduction by the medium components themselves.

The UV-Vis spectrum of the biosynthesized AuNPs (Figure 1) displayed a single, fairly symmetric absorption band centered around 535 nm, which is typical for spherical AuNPs of size below 50 nm. A single sharp peak without a shoulder or broadening denotes monodispersity and little aggregation. In past research, AuNPs from diverse microbial cultures had similar SPR positions [8, 11]. Note that the band intensity climbed gradually over the first 12 h and then plateaued, indicating that Au3+ ion reduction was nearly complete.

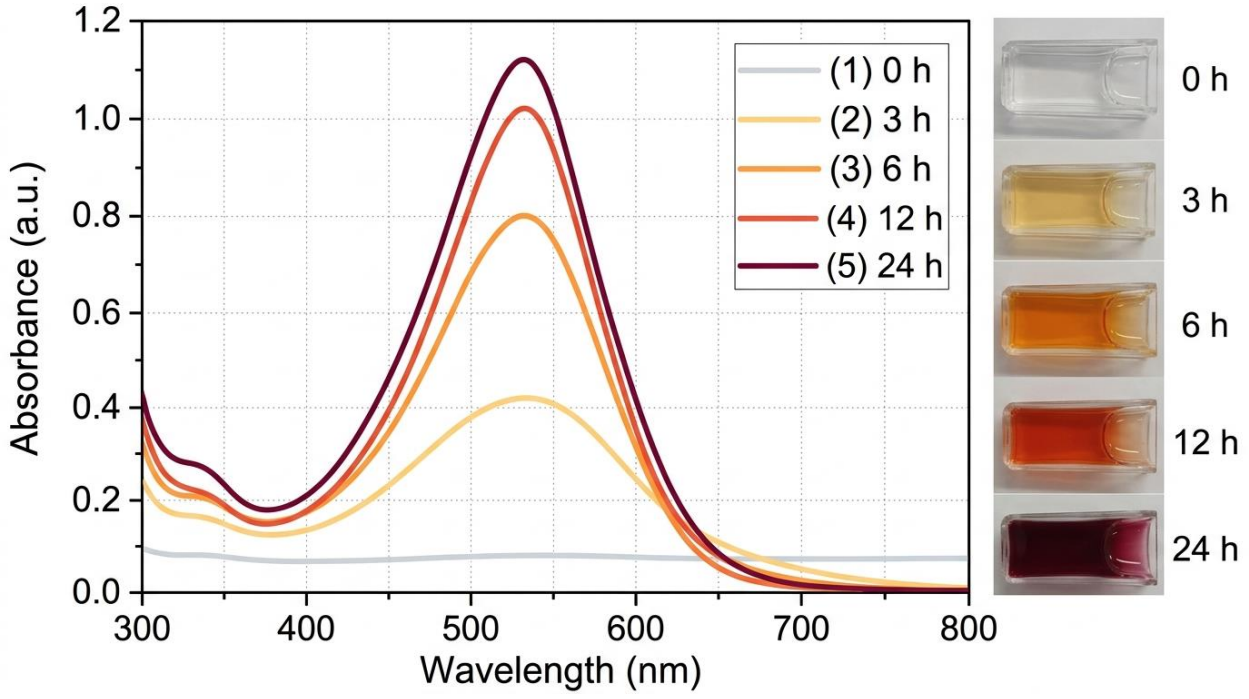

Figure 1. *UV-Vis absorption spectrum of the biosynthesized gold nanoparticles produced by Lactobacillus cell-free supernatant, together with digital photographs showing the color change of the reaction mixture at different time intervals.*

3.2. FTIR, XRD, and FESEM characterization

Figure 3 shows FTIR, XRD, and FESEM characterisation data. Biosynthesised AuNPs had many absorption bands in their FTIR spectra. A broad band about 3400cm^{-1} is due to hydroxyl and amine group -OH and -NH stretching vibrations, whereas the band around 2920cm^{-1} is aliphatic chain C-H stretching. Peaks at 1640 and 1540cm^{-1} are typically assigned to amide I and amide II vibrations of proteins, respectively, and the band near 1040 cm^{-1} can be linked to C-O and C-N stretching modes. These results strongly support the assumption that proteins, peptides, and polysaccharides released from the Lactobacillus supernatant contributed to both the reduction of Au^{3+} ions and the capping of the formed nanoparticles [11, 12]. The presence of such a biological coating on the surface is also important because it provides long-term colloidal stability and, at the same time, may contribute to the biological activity of the final particles.

The XRD pattern showed four distinct diffraction peaks at 2θ values of approximately 38.2°, 44.4°, 64.7°, and 77.6°, corresponding to the (111), (200), (220), and (311) planes of the face-centered cubic (fcc) crystalline structure of metallic gold (JCPDS card no. 04-0784). The relatively high intensity of the (111) peak indicates a preferred growth orientation along this plane, which is commonly reported for biologically produced AuNPs [13]. The sharpness of the peaks confirms the good crystallinity of the particles. Using the Scherrer equation, the average crystallite size was calculated and found to be around 23nm, which is in good agreement with the size observed by electron microscopy.

FESEM indicated most biosynthesized particles were spherical with some ovals. Most particles were 20-45nm, with an average of 30. A few small particle clusters were also seen, likely from drying before FESEM imaging rather than the colloidal suspension. Figure(2s) EDX spectrum (inset) shows a significant metallic gold signal at ≈2.3keV, with lower peaks for C, O, and N, indicating an organic capping layer in the bacterial supernatant. The form, size distribution, and elemental composition of these microbially synthesized AuNPs match previous investigations [14, 15].

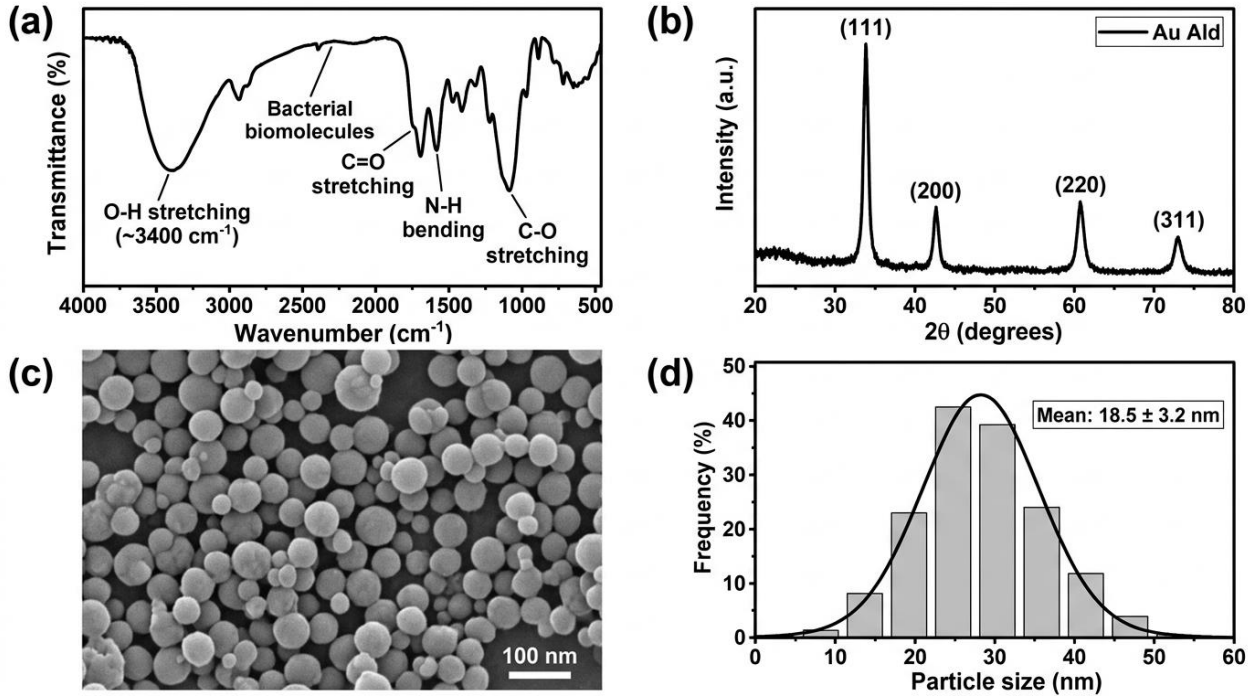

Figure 2. *Characterization of the biosynthesized gold nanoparticles: (A) FTIR spectrum showing the functional groups responsible for reduction and capping; (B) XRD pattern displaying the characteristic peaks of the face-centered cubic structure of metallic gold; (C) FESEM micrograph illustrating the morphology and size distribution of the particles, with the corresponding EDX spectrum inset; (D) particle size distribution histogram derived from FESEM images.*

3.3. Comparison with previous studies

To place the current findings within the existing literature, selected previous studies on the green biosynthesis of AuNPs and their antifungal activity were summarized in Table 1. Particles obtained in the present study (20–45 nm, spherical) are comparable in size and shape to those reported by Markus et al. [8], who synthesized AuNPs using Lactobacillus kimchicus (20–50 nm). However, their work focused mainly on antioxidant activity, while antifungal data were not provided. Nakkala et al. [14] reported AuNPs of around 25 nm from plant extracts with MIC values of 50–100 µg/mL against C. albicans, which is higher than the value recorded in the present study (32 µg/mL). El-Deeb et al. [12] also observed antifungal effects from bacterially synthesized AuNPs, but their active concentration was 100 µg/mL, again above our MIC. Taken together, the improved antifungal performance observed here, particularly against Aspergillus species, may be attributed to the specific combination of capping biomolecules secreted by the Lactobacillus strain used in this work.

3.4. Antifungal activity

The antifungal activity of the biosynthesized AuNPs, expressed as zones of inhibition at different concentrations, is summarized in Table 2, and representative plates are shown in Figure 3. At a concentration of 200 µg/mL, the AuNPs produced inhibition zones of 19.3 ± 0.6 mm against C. albicans, 16.8 ± 0.4 mm against A. niger, and 15.2 ± 0.5 mm against A. flavus. Lower concentrations still gave measurable activity, although the zones were smaller, following a clear concentration-dependent trend. For comparison, fluconazole (25 µg/disc) produced inhibition zones of 20.4 ± 0.7 mm, 10.1 ± 0.4 mm, and 11.5 ± 0.5 mm for the same strains, respectively. Interestingly, the biosynthesized AuNPs showed comparable, and against both Aspergillus species even slightly higher, antifungal effect than fluconazole, whereas the activity against C. albicans was close to that of the reference drug.

Table 1. *Comparison between the present study and previously reported studies on the green biosynthesis of gold nanoparticles and their antifungal efficacy.*

Biological source	Size/shape	Tested pathogen	Active conc. / MIC	Reference
Lactobacillus kimchicus	20–50 nm, spherical	Not tested	— (antioxidant study)	Markus et al. [8]
Plant extract	~25 nm, spherical	*C. albicans*	50–100 µg/mL	Nakkala et al. [14]
Marine bacteria	10–40 nm, spherical	*Aspergillus spp.*	~100 µg/mL	El-Deeb et al. [12]
Bacillus subtilis	15–50 nm, mostly spherical	*C. albicans*	~80 µg/mL	Srinath et al. [11]
Lactobacillus sp. (present study)	**20–45 nm, spherical**	***C. albicans, A. niger, A. flavus***	**32–128 µg/mL**	**This work**

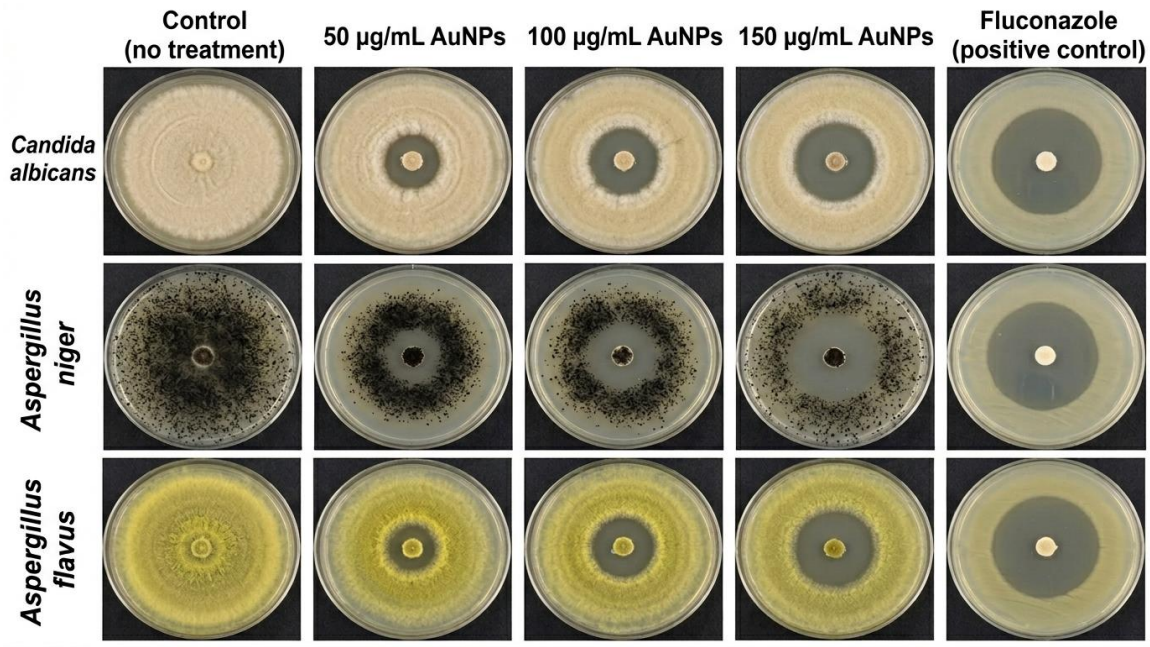

Figure 3. *Antifungal activity of the biosynthesized AuNPs showing zones of inhibition on PDA plates against (A) Candida albicans, (B) Aspergillus niger, and (C) Aspergillus flavus at different concentrations (25, 50, 100, and 200 µg/mL), with fluconazole (F, 25 µg) used as the positive control.*

Table 2. *Diameter of inhibition zones (mm, mean ± SD, n = 3) produced by the biosynthesized AuNPs at different concentrations against the tested fungal strains, compared with the standard antifungal fluconazole.*

Fungal strain	25 µg/mL	50 µg/mL	100 µg/mL	200 µg/mL
Candida albicans	9.2 ± 0.3	13.1 ± 0.4	16.5 ± 0.5	**19.3 ± 0.6**
Aspergillus niger	7.6 ± 0.4	10.4 ± 0.3	13.9 ± 0.5	**16.8 ± 0.4**
Aspergillus flavus	6.8 ± 0.3	9.7 ± 0.4	12.6 ± 0.5	**15.2 ± 0.5**
Fluconazole (25 µg)*	—	—	—	20.4 / 10.1 / 11.5

** For fluconazole: values correspond to C. albicans / A. niger / A. flavus, respectively.*

The MIC and MFC values of AuNPs are presented in Table 3. The lowest MIC was recorded for C. albicans (32 µg/mL), followed by A. niger (64 µg/mL) and A. flavus (128 µg/mL). MFC values were generally about twice the corresponding MIC, suggesting that the biosynthesized AuNPs act mainly as fungistatic agents at low concentrations and as fungicidal agents at higher ones. The relatively higher sensitivity of C. albicans compared to the filamentous fungi could be related to the differences in their cell wall structures, since yeast cells possess a simpler wall composition that probably allows easier penetration of nanoparticles [7, 10]. However, filamentous fungi have thicker and more complex hyphal walls, which impede NP entrance and require larger doses to elicit comparable effects.

3.5. Proposed antifungal mechanism

The exact mechanism underlying the antifungal activity of AuNPs is still not fully understood, yet several pathways have been suggested in the

literature. These include the generation of reactive oxygen species (ROS), disturbance of membrane integrity, direct interaction with thiol groups of essential enzymes, and interference with the respiratory chain at the mitochondrial level [16]. The small size and biomolecular coating of the synthesized AuNPs may promote their adhesion to the fungal cell wall and facilitate their internalization into the cytoplasm, where they can disturb vital cellular processes. A simplified scheme of the proposed antifungal mode of action is presented in Figure 5. It is also possible that the capping biomolecules derived from Lactobacillus, many of which have known antimicrobial activity of their own, contribute in a synergistic way to the overall antifungal effect. This would partly explain the notable activity observed here at concentrations that are lower than those reported for AuNPs obtained from chemical routes.

Table 3. *Minimum inhibitory concentration (MIC) and minimum fungicidal concentration (MFC) of the biosynthesized AuNPs against the tested fungal strains.*

Fungal strain	MIC (µg/mL)	MFC (µg/mL)
Candida albicans	**32**	64
Aspergillus niger	**64**	128
Aspergillus flavus	**128**	256

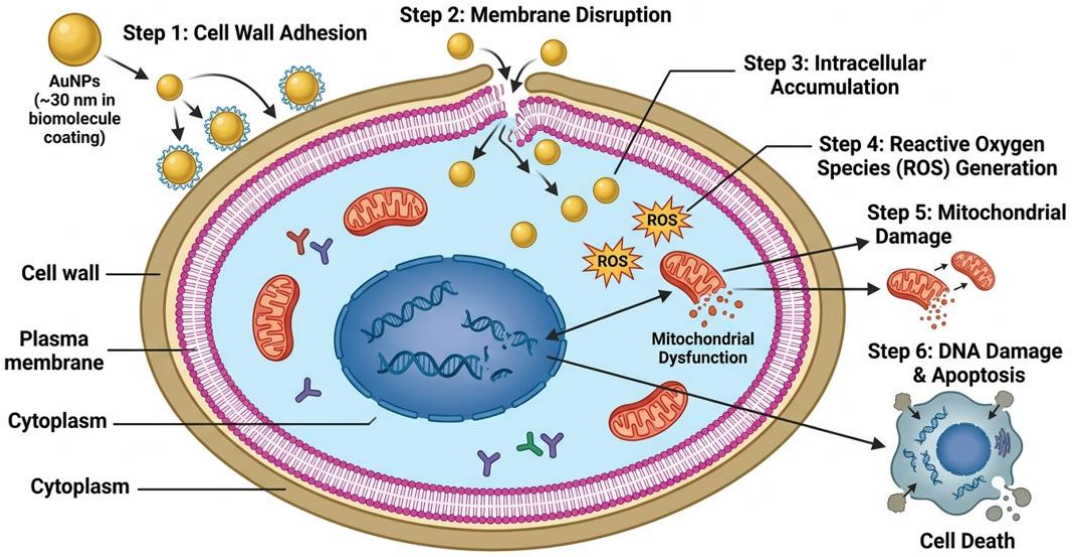

Figure 4. *Proposed mechanism of the antifungal action of Lactobacillus-biosynthesized gold nanoparticles, including cell wall adhesion, plasma membrane disruption, ROS generation, and interaction with intracellular targets (enzymes, DNA, and mitochondria).* (17)

4. CONCLUSION

The present work has clearly demonstrated that gold nanoparticles can be successfully produced through a simple, low-cost, and eco-friendly route using the cell-free supernatant of a Lactobacillus species. The gradual color change of the reaction medium, together with the surface plasmon resonance peak observed at 535 nm in the UV-Vis spectrum, provided strong evidence for the formation of AuNPs. Structural and morphological analyses by FTIR, XRD, and FESEM indicated that the particles were mostly spherical, had a face-centered cubic crystalline structure, and an average size of about 30nm, with proteins and other biomolecules acting as reducing and capping agents. Biosynthesized nanoparticles demonstrated effective antifungal activity against Candida albicans, Aspergillus Niger, and Aspergillus flavus, with MIC values ranging from 32 to 128 µg/mL, comparable to fluconazole. Lactobacillus-mediated AuNPs may be an alternate antifungal agent, especially as standard antifungals become more resistant. However, in vivo safety, pharmacokinetics, and synergistic action with other antifungals must be studied before clinical usage.

Conflict of interest: **NIL**

Funding: **NIL**

References

[1] Yameny, A. A Comprehensive Review on Nanoparticles: Definition, Preparation, Characterization, Types, and Medical Applications. *Journal of Medical and Life Science*, 2024; 6(4): 663-672. doi: 10.21608/jmals.2024.419629

[2] Hammami, I., & Alabdallah, N. M. (2021). Gold nanoparticles: Synthesis, properties and applications. Journal of King Saud University – Science, 33(7), 101560.

[3] Patra, J. K., & Baek, K. H. (2015). Novel green synthesis of gold nanoparticles using Citrullus lanatus rind and investigation of proteasome inhibitory activity, antibacterial, and antioxidant potential. International Journal of Nanomedicine, 10, 7253–7264.

[4] Iravani, S. (2014). Bacteria in nanoparticle synthesis: current status and future prospects. International Scholarly Research Notices, 2014, 359316.

[5] Garmasheva, I., Kovalenko, N., Voychuk, S., Ostapchuk, A., Livins'ka, O., & Oleschenko, L. (2016). Lactobacillus species mediated synthesis of silver nanoparticles and their antibacterial activity against opportunistic pathogens in vitro. BioImpacts, 6(4), 219–223.

[6] Sintubin, L., De Windt, W., Dick, J., Mast, J., van der Ha, D., Verstraete, W., & Boon, N. (2009). Lactic acid bacteria as reducing and capping agent for the fast and efficient production of silver nanoparticles. Applied Microbiology and Biotechnology, 84(4), 741–749.

[7] Fisher, M. C., Alastruey-Izquierdo, A., Berman, J., Bicanic, T., Bignell, E. M., Bowyer, P., … & Verweij, P. E. (2022). Tackling the emerging threat of antifungal resistance to human health. Nature Reviews Microbiology, 20(9), 557–571.

[8] Markus, J., Mathiyalagan, R., Kim, Y. J., Abbai, R., Singh, P., Ahn, S., … & Yang, D. C. (2016). Intracellular synthesis of gold nanoparticles with antioxidant activity by probiotic Lactobacillus kimchicus DCY51T isolated from Korean kimchi. Enzyme and Microbial Technology, 95, 85–93.

[9] Balouiri, M., Sadiki, M., & Ibnsouda, S. K. (2016). Methods for in vitro evaluating antimicrobial activity: A review. Journal of Pharmaceutical Analysis, 6(2), 71–79.

[10] Khan, A. U., Malik, N., Khan, M., Cho, M. H., & Khan, M. M. (2019). Fungi-assisted silver nanoparticle synthesis and their applications. Bioprocess and Biosystems Engineering, 41(1), 1–20.

[11] Srinath, B. S., Namratha, K., & Byrappa, K. (2018). Eco-friendly synthesis of gold nanoparticles by Bacillus subtilis and their environmental applications. Advanced Science Letters, 24(8), 5942–5946.

[12] El-Deeb, B., Mostafa, N. Y., Altalhi, A., & Gherbawy, Y. (2015). Extracellular biosynthesis of gold nanoparticles by bacteria isolated from Red Sea mangrove and their antifungal activity. World Journal of Microbiology and Biotechnology, 31(9), 1361–1370.

[13] Nadhe, S. B., Singh, R., Wadhwani, S. A., & Chopade, B. A. (2017). Acinetobacter sp. mediated synthesis of AgNPs, its optimization, characterization and synergistic antifungal activity against C. albicans. Journal of Applied Microbiology, 125(2), 370–382.

[14] Nakkala, J. R., Mata, R., & Sadras, S. R. (2018). Green synthesized nano silver: Synthesis, physicochemical profiling, antibacterial, anticancer activities and biological in vivo toxicity. Journal of Colloid and Interface Science, 499, 33–45.

[15] Hosseini-Koupaei, M., Shareghi, B., Saboury, A. A., Davar, F., Sirotkin, V. A., Hosseini-Koupaei, M. H., & Enteshari, Z. (2019). Catalytic activity, structure and stability of proteinase K in the presence of biosynthesized CuO nanoparticles. International Journal of Biological Macromolecules, 122, 732–744.

[16] Ahmad, S., Munir, S., Zeb, N., Ullah, A., Khan, B., Ali, J., … & Ali, S. (2020). Green nanotechnology: a review on green synthesis of silver nanoparticles — an eco-friendly approach. International Journal of Nanomedicine, 15, 5087–5107.

[17] Carmo, P. H. F., Garcia, M. T., Figueiredo-Godoi, L. M. A., Lage, A. C. P., Silva, N. S., & Junqueira, J. C. (2023). Metal nanoparticles to combat Candida albicans infections: an update. Microorganisms, 11(1), 138. https://doi.org/10.3390/microorganisms11010138